GEOPHYSICAL RESEARCH LETTERS, VOL. ???, XXXX, DOI:10.1029/,

The relationship between sea-level and bottom pressure variability in an eddy permitting ocean model

Rory J. Bingham

Proudman Oceanographic Laboratory, Liverpool, U.K.

Chris W. Hughes

Proudman Oceanographic Laboratory, Liverpool, U.K.

Rory J. Bingham, Chris W. Hughes, Proudman Oceanographic Laboratory, 6 Brownlow St., Liverpool L3 5DA, U.K. (rjbi@pol.ac.uk, cwh@pol.ac.uk)

We investigate the relationship between sea-level (after application of an inverse-barometer correction) and ocean bottom pressure, in an eddy-permitting ocean model. We find that the presence of eddies can disrupt this relationship even on timescales as short as 10–20 days, but only in the regions of most energetic eddy variability. Away from eddies, the relationship is similar to that seen in a coarser-resolution model, with a tight relationship between sea-level and bottom pressure at high frequencies, but with significant correlations between sea-level and bottom pressure at interannual timescales seen only in shelf sea regions. In the deep ocean, regions where sea-level and bottom pressure remain related out to the longest timescales are in the Arctic Ocean and regions of the Southern Ocean, where particularly large amplitude barotropic fluctuations are found but where the mesoscale signal is weak.

1. Introduction

In combination, altimetry and a satellite gravity mission such as GRACE have the potential to distinguish between barotropic and baroclinic sea-level changes and thereby shed new light on the physics of the ocean. *Jayne et al.* [2003] for instance shows how the two could be combined to determine changes in ocean heat storage. Regarding ocean bottom pressure derived from GRACE observations, however, we are still at the validation stage where (with some circularity) we wish to use altimetry to make inferences regarding the expected GRACE signal. To this end, in a recent paper *Vinogradova et al.* [2007] (henceforth VPS) investigated the relationship between sea-level and bottom pressure variability in the coarse (1°) resolution ocean model ECCO. They found strong equivalence between model sea-level and bottom pressure at periods <30 days, while at periods up to 100 days the the strong equivalence was generally confined to shallow seas and at high latitudes (>60°). At longer periods little correspondence was found between sea-level and bottom pressure.

However, on smaller scales the ocean and sea-level, particularly in regions of strong currents, are dominated by mesoscale eddies, and this is in fact where the majority of the ocean's kinetic energy lies [*Fu and Smith*, 1996]. For this reason coarse resolution models tend to underestimate, quite drastically in some cases, the sea-level variance in comparison with what is measured by altimetry. Therefore, since these eddies are generally baroclinic, the strong correspondence in sea-level and bottom pressure reported by VPS may well be an artifact of the coarse, non-eddy permitting resolution of their model (a point raised by VPS themselves). In this paper, therefore, we extend the VPS analysis to an eddy resolving ocean model, also with realistic forcing, attempting to replicate the analysis of VPS as closely as possible.

2. Model description

The main results of this paper are based on an analysis of the Ocean Circulation and Climate Advanced Modelling project model (OCCAM) run at the National Oceanography Centre, Southampton. It is a global, z-level, free surface model with a rotated grid over the North Atlantic, and is forced with 6-hourly ECMWF atmospheric data. The run we are considering (run 202) is at 0.25°resolution, with 66 vertical levels, and covers the 19-year period 1985-2003, with an initial 4 years of spin-up [*Coward and de Cuevas*, 2005]. The data is output as five day means. We apply an inverse barometer correction to the model sea-level, as the forcing (unlike in VPS) includes atmospheric pressure.

3. Results

Compared with the coarse resolution ECCO model used by VPS, at the eddy permitting resolution of OCCAM the regions of high sea-level variability are more clearly associated with regions of strong currents, particularly noticeable along the Gulf-Stream and North Atlantic Current (NAC), the Antarctic Circumpolar Current (ACC) and the Agulhas retro-reflection (Figure 1a). Moreover, the amplitude is several centimetres greater, achieving values in excess of 15cm. This is in spite of the fact that we are using five day means, for which some high frequency power is lost, rather than the daily mean values used by VPS. This confirms the view that mesoscale eddy variability, generated in regions of baroclinic instability, makes a significant contribution to the sea-level anomaly field.

The ability of a model to permit eddies has a much smaller influence on bottom pressure than is the case for sea-level, both in terms of overall structure and amplitude (Figure 1b). This supports the idea that the regions of high variability seen in the OCCAM sea-level map are due primarily to baroclinic eddies. Within the large regions of coherent bottom pressure fluctuations in the Southern Ocean and the North Pacific, bottom pressure deviations are up to 1-2cm less in OCCAM compared with the VPS model, but have a similar form, being, as they are, defined by topographic contours [*Webb and de Cuevas*, 2002a, b; *Bingham and Hughes*, 2006]. Since bottom pressure fluctuations generally have significant power at periods less than five days this is most likely due to the fact that the OCCAM data have been averaged over a longer time span. Although in terms of sea-level the Arctic does not stand out as a region of especially high variability, in terms of bottom pressure it does. A similar signal in a barotropic version of OCCAM and observational evidence for it was presented by *Hughes and Stepanov* [2004]. The boundary of this signal is sharply defined by the topography of the Greenland-Scotland Ridge between the North Atlantic and Nordic Seas and the shelf in the Bering Strait, and most likely represents a trapped geostrophic mode similar to those found in the Southern Ocean. As in the VPS model, the greatest bottom pressure amplitudes are found in shallow shelf seas.

Following VPS we quantify the extent to which sea-level anomalies are barotropic by computing the correspondence between sea-level h' and bottom pressure p'_b anomalies (the latter expressed in sea-level units by multiplying by a reference density and acceleration due to gravity), defined as:

$$s = \frac{< h' - p'_b >}{< h' >}, \tag{1}$$

where angle brackets represents variance of the term enclosed by them. Clearly a score of $s = 0$ would indicate that sea-level variability is entirely barotropic. The map of s is shown in Figure 1c. The predominance of yellow to red colours shows that over most of the open ocean baroclinic variability dominates. Only in the Arctic basin, the shallow shelf seas, and some isolated patches of the Southern Ocean does barotropic variability dominate when all timescales are considered. The pattern is similar to that found in the ECCO model used by VPS. This is because the presence of eddies only weakens the relationship between sea-level and bottom pressure in regions where most of the large-scale sea-level variance is, in any case, weakly coupled to bottom pressure.

Next we consider how the relationship between sea-level and bottom pressure depends on latitude and on the water depth as a function of frequency. Cross-spectral analysis provides an appropriate means to do this. The mean admittance between sea-level and bottom pressure anomalies over a particular geographic interval (as shown in Figure 2) is defined by

$$Z(\omega) = \frac{\overline{\hat{h}'\hat{p}_b'^{*}}}{\overline{\hat{h}'\hat{h}'^{*}}}, \qquad (2)$$

where $\hat{x}$ represents the Fourier transform of x, and $\overline{x}$ represents the mean of x. Motivated by Figure 1c which shows clearly the much closer relationship between sea-level and bottom pressure over the shelf-seas compared with the deep ocean we compute the mean admittance for shallow (<200m) and deep (>1000m) parts of the ocean separately (see Figure 2a). At the Nyquist frequency (0.1 cpd) the amplitude of the admittance is 1 indicating the variability on the shelf is essentially barotropic. As we move to lower frequencies the amplitude declines, but always remains greater than 0.8, showing that even on multi-year timescales baroclinic processes do not strongly decouple sea-level from bottom pressure in shallow water. The similarity to the result from ECCO presented by VPS is to be expected as eddies are not the dominant source of sea-level variability on the shelves.

A much greater difference between ECCO and OCCAM is seen we we consider the admittance between sea-level and bottom pressure over the deep ocean. We now see clearly the influence of eddies. Like the variability on the shelf, at the highest resolvable frequencies the deep ocean in OCCAM is primarily barotropic, as it is in ECCO. And in both models, the admittance amplitude falls away much more rapidly than is the case in shallow water, indicating the importance of baroclinic processes in the deep ocean. However, the roll-off is much steeper in OCCAM. In OCCAM the amplitude falls to below 0.2 for periods greater than 100 days, while for ECCO the amplitude is 0.5 at 100 days, and even for much longer periods it remains above 0.4. This implies that in OCCAM the baroclinic nature of sea-level variability over the deep ocean comes to prominence at relatively high frequencies compared with ECCO. This is consistent with the expected effect of mesoscale eddies, which are absent from ECCO and which locally weaken the relationship between sea-level and bottom pressure.

In Figure 2a we also address the question of whether the presence of eddies disrupts the relationship between sea-level and bottom pressure over the deep ocean at larger scales. Forming 1°or 2°box averages does little to change the spectral relationship between the two fields. This shows that mesoscale eddies contribute to the sea-level variability at length-scales greater than the resolution that is required for them to be present in the model, and we cannot recover a relationship between sea-level and bottom pressure similar to that found in ECCO simply by averaging the high resolution field to the resolution of ECCO. In fact it is not until we average over 8°bins that a relationship similar to that reported by VPS is seen.

Figure 1c shows that, when considered over all frequencies taken together, the variability in the deep ocean at high latitudes tends to be more barotropic than at lower latitudes. We therefore now consider how the relationship in the tropics (0°to 15°), the mid-latitudes (45°to 60°), and high latitudes (60°to 80°) depends on frequency (see Figure 2b). It is clear from Figure 2b that the variability in any particular frequency band becomes more barotropic as we move progressively poleward, just as was the case for the ECCO model used by VPS. Whilst at the Nyquist frequency the variability in both mid- and high-latitudes bands is essentially barotropic, in the tropics sea-level variability, even at the highest resolvable frequencies, includes significant baroclinic variability. Just as for the deep ocean taken it is entirety, the individual latitude bands each show a more rapid decline in barotropic variability relative to baroclinic variability, compared with the ECCO model. However, the decline in the barotropic to baroclinic ratio occurs more slowly at higher latitudes. In general, at all latitudes the ocean is less barotropic in OCCAM than it is in ECCO.

To test the hypothesis that the more rapid decline in barotropic variability in OCCAM compared with ECCO is due to eddies we recompute the cross-spectra for the mid- and high-latitude bands but with further partitioning between regions of low (sd<5cm) and high (sd>10cm) sea-level variability. As Figure 3c shows, over regions of low sea-level variability, indicative of regions of little eddy activity, our cross-spectra look much more like those found in ECCO. The variability remains barotropic to longer timescales, than was the case for the zonal bands considered in their entirety, particularly for the mid-latitude band. The roll-off is also more gradual, although the final amplitudes are still somewhat less than for the ECCO model. On the other hand, the cross-spectra for the regions of high sea-level variability, indicative of greater eddy activity, appear as more extreme versions of the corresponding spectra of Figure 2b. Even at the Nyquist frequency the variability is significantly different from barotropic and the reduction in the barotropic to baroclinic energy ratio is much more rapid than in the low variability regions. The main difference between mid and high latitudes is that there is a larger fraction of the domain in the mid-latitude band occupied by eddies.

Finally, we consider the geographical patterns of admittance partitioned by frequency band (as shown in Figure 3). This is defined by summing over the required band before calculating the complex product (rather than computing the average of the complex products as in equation 2):

$$Z(\omega) = \frac{\overline{\hat{h}'}\,\overline{\hat{p}_b'}^{*}}{\overline{\hat{h}'}\,\overline{\hat{h}'}^{*}}. \tag{3}$$

Using the ECCO model, VPS found that in the 1–20 cpd frequency band the ocean behaved everywhere outside the tropics as a barotropic fluid. In OCCAM too, we find that over most of the extra-tropical ocean in the 10–20 cpd frequency band the ocean behaves barotropically (see Figure 3a). However, unlike ECCO, even at these high frequencies the close correspondence between sea-level and bottom pressure breaks down in the regions where there are strong currents, such as the Gulf-Stream, Kuroshio, Agulhas, and the

ACC. These are regions where the sea-level variability is greatest. Moving to the 20-60cpd band (see Figure 3b) the picture is again in broad terms as it is with ECCO. The tropical region of decoherence in the deep ocean has now spread to higher latitudes by several degrees and the small regions of decoherence associated with the strong currents, seen at the highest frequencies, have grown and spread along the extensions in the case of the Kuroshio and Gulf-Stream. This growth of decoherence is much less pronounced in the ECCO model, a result of not representing baroclinic eddies that are produced in these regions. Note also how, in addition to the energetic western boundary regions, there are thin regions of decoherence at other ocean boundaries. This may be a result of the propagation of waves with baroclinic structure along the shelf slope, or it may reflect the fact that interactions with this steep topography introduces shorter length scales, which results in a shorter time being necessary for baroclinic effects to become important (see the scaling given by *Gill and Niiler* [1973]). At seasonal timescales, over the open ocean, it is only some small isolated patches of the Southern Ocean and in the Arctic that remain coherent in OCCAM. Similarly in ECCO it is the Southern Ocean and Arctic Ocean where the signal remain coherent, although for the Southern Ocean the coherence is somewhat stronger than it is in OCCAM. ECCO also shows greater coherence in the South Pacific in comparison to OCCAM.

In Figure 3d we extend the analysis to interannual time periods where we find that over the open ocean variability is dominated by baroclinic processes. That is not to say that barotropic processes are not at work, only that they are weak when compared with the baroclinic processes. Strong coherence between sea-level and bottom pressure remains at inter-annual timescales only on the shallow shelf seas, most noticeably in the Arctic, but also on the Northwest European shelf, on the western sides of both Atlantic and Pacific oceans, and close to Antarctica.

4. Discussion

Taken together, the results of VPS and this study suggest the following interpretation. Barotropic fluctuations occur throughout the ocean, but are most clearly seen at relatively short timescales. This is because the link between sea-level and bottom pressure is broken by baroclinic fluctuations which tend to dominate at longer timescales. The timescale at which the baroclinic effects become important depends particularly on length scale, and on the relative amplitudes of the excited baroclinic and barotropic variations. So, in regions where short length scale eddies are most energetic, the decoupling occurs even at periods as short as 10–20 days, spreading at longer timescales to broader regions with substantial mesoscale variability. Similarly, bottom pressure and sea-level variability become decoupled relatively quickly over the steep continental slopes, where length scales are naturally short. Regions in which bottom pressure and sea-level remain coupled to relatively long periods, such as the Arctic and some regions of the Southern Ocean, correspond to regions of particularly energetic barotropic fluctuations and particularly weak mesoscale variability. Even here, however, little coherence remains at interannual periods. At such periods, coherence only remains in shelf sea regions, where the barotropic fluctuations are especially large, and where the shallow depth means that larger density variations are needed to compensate the sea-level variations. Another special case is the tropical band where, as a result of the more rapid propagation of waves at low latitudes, baroclinic variability becomes important at shorter timescales although, again, this occurs at shorter timescales for fluctuations at short length scales than for those at longer length scales. Our study provides no reason to believe that the presence of eddies disrupts the relationship between sea-level and bottom pressure, other than in the obvious way that sea-level and bottom pressure are only weakly coupled in the eddies themselves.

For comparison of sea-level from altimetry with bottom pressure from GRACE, we find that it is necessary to average over about 8° in order to retain a strong correlation out to a period of 100 days. That is with perfect sea-level data; with the sampling permitted by altimetry it is not clear whether even such large-scale averaging would be sufficient to filter out the mesoscale signal. An alternative, as we show in Fig. 2c, is to compare sea-level and bottom pressure in regions with relatively small sea-level variance.

Acknowledgments. This study was supported by the UK NERC thematic RAPID programme, NER/T/S/2002/00439 and NER/T/S/2002/00485, and represents a contribution to the Proudman Oceanographic Laboratory's "Geodetic oceanography, polar oceanography and sea level" Programme, a part of Oceans2025.

References

Bingham, R. J., and C. W. Hughes (2006), Observing seasonal bottom pressure variability in the North Pacific with GRACE, *Geophys. Res. Lett.*, *33*, L08607, doi: 10.1029/2005GL025489.

Coward, A., and B. de Cuevas (2005), The OCCAM 66 Level Model: physics, initial conditions and external forcing., *Internal report 99*, SOC, 58pp, available from *http://www.noc.soton.ac.uk/JRD/OCCAM/OCCAM-p25k66-run202.pdf.*

Fu, L., and R. Smith (1996), Global ocean circulation from satellite altimetry and high-resolution computer simulation, *Bull. Amer. Meteor. Soc.*, *77*, 2625–2636.

Fukumori, I. (1995), Assimilation of TOPEX sea level measurements with a reduced-gravity, shallow water model of the tropical Pacific Ocean, *J. Geophys. Res.*, *100*(C12), 25,027–25,040.

Hughes, C. W., and V. Stepanov (2004), Ocean dynamics associated with rapid J_2 fluctuations: Importance of circumpolar modes and identification of a coherent Arctic mode, *J. Geophys. Res.*, *109*, C06002, doi:10.1029/2003JC002176.

Gill, A. E. and P. P. Niiler (1973), The theory of the seasonal variability in the ocean, *Deep Sea Res. Oceanogr. Abstr.*, *20*, 141–177.

Jayne, S., J. Wahr, and F. Bryan (2003), Observing ocean heat content using satellite gravity and altimetry, *J. Geophys. Res.*, *108*(C2), 3031, doi:10.1029/2002JC001619.

Vinogradova, N. T., R. Ponte, , and D. Stammer (2007), Relation between sea level and bottom pressure and the vertical dependence of oceanic variability, *Geophys. Res. Lett.*, *34*, L03608, doi:10.1029/2006GL028588.

Webb, D., and B. de Cuevas (2002a), An ocean resonance in the Southeast Pacific, *Geophys. Res. Lett.*, *29*(8), 1252, doi:10.1029/2001GL014259.

Webb, D., and B. de Cuevas (2002b), An ocean resonance in the Indian sector of the Southern Ocean, *Geophys. Res. Lett.*, *29*(14), 1664, doi:10.1029/2002GL015270.

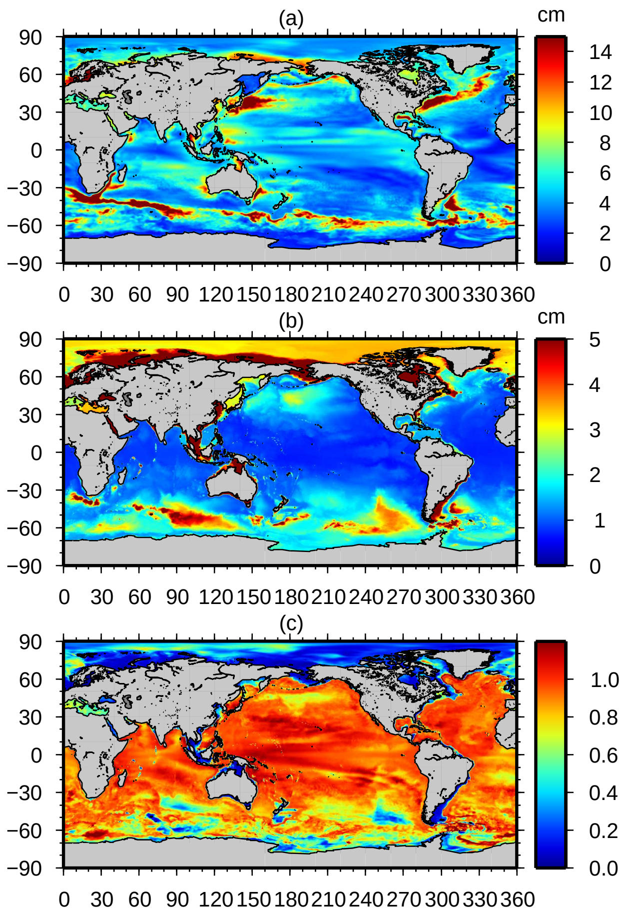

Figure 1. (a) The standard deviation of detrended model sea-level anomalies. (b) The standard deviation of detrended model bottom pressure anomalies. (c) The correspondence between model sea-level and bottom pressure anomalies, where a perfect correspondence gives a score of zero.

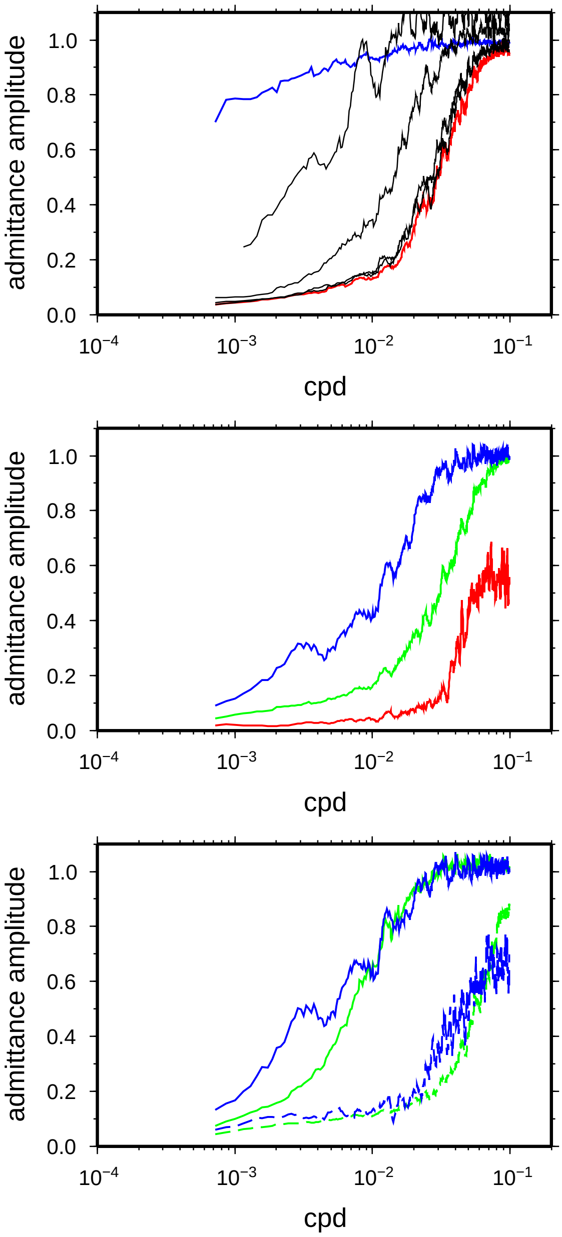

Figure 2. (a) The amplitude admittance between model sea-level and bottom pressure anomalies partitioned between shallow (<200m) (blue) and deep (>1000m). The admittance for the deep ocean for averaging over 1°, 2°, 4°, and 8°(black). (b) The amplitude admittance for the deep ocean partitioned between tropical (0-15°) (red), mid-latitudes (45-60°) (green), and high-latitudes (60-80°). (c) As in (b) but the mid- and high- latitude bands further partitioned between low (<5cm) sea-level standard deviation (solid lines) and high (>10cm) sea-level standard deviation.

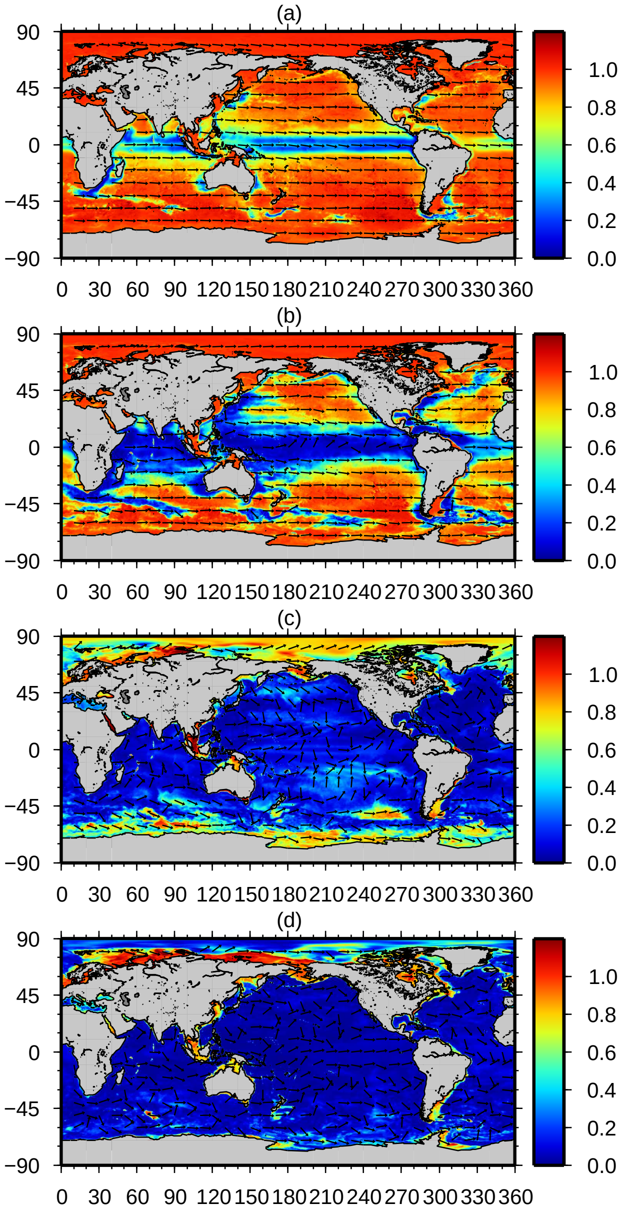

Figure 3. The admittance amplitude and phase between model sea-level and bottom pressure anomalies partitioned between (a) 10-20cpd, (b) 20-60cpd, (c) annual, and (d) inter-annual frequency bands. Zero phase difference is indicated by an eastward pointing vector.